Chinese Chemical Letters 32 (2021) 1451–1455

Contents lists available at ScienceDirect

Chinese Chemical Letters

journal homepage: www.elsevier.com/locate/cclet

Communication

Intermetallic PdBi aerogels with improved catalytic performance for the degradation of organic pollutants in water

Xiaofeng Tan[a,1], Jun Qin[b,1], Yan Li[c], Yuting Zeng[c], Jindi Gong[c], Gengxiu Zheng[a,**], Feng Feng[b,**], He Li[a,c,*]

[a] School of Chemistry and Chemical Engineering, University of Jinan, Ji'nan 250022, China
[b] College of Chemistry and Environmental Engineering, Shanxi Datong University, Datong 037009, China
[c] College of Optoelectronics Technology, Chengdu University of Information Technology, Chengdu 610225, China

ARTICLE INFO

Article history:
Received 27 June 2020
Received in revised form 27 July 2020
Accepted 23 September 2020
Available online 24 September 2020

Keywords:
PdBi aerogels
Degradation
Organic micropollutants
Atom utilization ratio
Synergistic effect

ABSTRACT

It is always highly pursued to develop efficient and durable catalysts for catalytic applications. Herein, intermetallic PdBi aerogels with tunable activity were prepared successfully *via* a surfactant-free spontaneous gelation process. The prepared PdBi aerogels have a three-dimensional high porous structure and plentiful active sites pervaded on the ultrathin interlinked nanowires network. These unique structures, as well as the synergistic effect between Pd and Bi, can accelerate mass and electron transfer, and improve the atom utilization ratio of Pd atoms to promote the catalytic efficiency. As a proof-of-concept application, the optimized Pd_2Bi_1 aerogels exhibit 4.2 and 6.2 times higher catalytic activity for the reduction of 4-nitrophenol (4-NP) and methylene blue (MB) than those of commercial Pd/C, respectively. With the introduction of non-noble metal of Bi, the cost of the resulted PdBi aerogels can be dropped significantly while the catalytic capability of PdBi aerogel will be improved sharply. This strategy will bring good hints to rationally design fine catalysts for various applications.

Metallic aerogels exhibited great potential in electrocatalysis [1,2] extended from ethanol oxidation to oxygen reduction reaction by virtue of the unique structure, which are interconnected colloidal nanocrystals with large-scale porous nanowires network [3]. However, rapid and straightforward preparation of metal aerogels with clear interfaces still faces enormous challenges due to the essential introduction of surfactant during the destabilizing gelation step. The residual surfactants adhered to the aerogels can influence the electron and mass transfer, and cause the decrease of the catalysis efficiency [4]. To overcome these limitations, a universal approach was recently proposed by using Cu as a linker for the preparation of bimetallic aerogels [5], in which Cu atoms can accelerate the gelation process to form a hydrogel. Also, another way is to achieve an accelerated gelation process by taking advantage of the crosslinking effects of dopamine [6]. Hence, optimizing the synthetic procedure with accelerated gelation kinetics will do help to gain more insight into macroscopic self-assembly and further extend their potential applications beyond electrocatalysis.

The intermetallic aerogels usually possess a nanowire-based backbone which is mainly involved in noble metals (Pd, Au, Pt, Ir) [7–10]. In order to cut down the cost of noble metal aerogels, to explore new hierarchical metallic aerogels with a variety of non-precious metals is of great interest. Therefore, bismuth (Bi), was first proposed to prepare intermetallic PdBi aerogels. As expected, Bi atoms exhibit a structure-directing function similar to the role of Cu and play a significant role in the formation of PdBi hydrogel.

Organic micropollutants will often do serious threats to human health although only containing a low concentration in water [11–13]. 4-Nitrophenol (4-NP) have high toxicity, carcinogenicity, and bioaccumulation, and been listed as priority pollutants by the US Environmental Protection Agency (USEPA) [14–18]. Methylene blue (MB) is also traditional contamination to the watery environment. So far, a plenty of strategies, such as adsorption [19], photocatalysis [20], oxidation [21] and catalytic reduction [22] were developed to remove these micropollutants. However, few studies have been done to check the application of intermetallic aerogels for catalytic reduction degradation of organic micropollutants. Here, 4-NP and MB were

* Corresponding author at: School of Chemistry and Chemical Engineering, University of Jinan, Ji'nan 250022, China.
** Corresponding authors.
E-mail addresses: chm_zhenggx@ujn.edu.cn (G. Zheng), feng-feng64@263.net (F. Feng), lihecd@gmail.com (H. Li).
[1] These authors contributed equally to this work.

https://doi.org/10.1016/j.cclet.2020.09.043
1001-8417/

chosen as model organic micropollutants [23–25]. For the first time, intermetallic PdBi aerogels with clear interfaces were prepared successfully through in situ reductions of $PdCl_4^{2-}$ and Bi^{3+} precursors by $NaBH_4$ (Fig. 1A). After optimization of the composition of PdBi aerogels, the resulted intermetallic PdBi aerogels exhibit superior catalytic performance for the degradation of 4-NP and MB. The excellent catalytic performance can be attributed to the following merits: (1) The self-supported interconnected networks provide a robust architecture against corrosion during catalysis; (2) the surfactant-free strategy avoids the adverse effect of surfactants on the surface of intermetallic catalysts; (3) the feature of advantageous 3D high-porosity provides a large specific surface area and interlinked channels for mass diffusion, which is beneficial to the adsorption of reactants and desorption of products; (4) the entire self-supported metallic backbone with interlinked ultrathin nanowires could provide free paths for efficient electron transfer, and the plentiful active sites pervaded on the nanowires can substantially boost catalytic activity toward organic micropollutants degradation. The exciting results would enrich our insights and broaden our horizons on the rational design of fine intermetallic aerogels based catalytic systems for environmental remediation and many other promising applications.

The structure and morphology of intermetallic PdBi aerogels were firstly investigated by scanning electron microscope (SEM). Three-dimensional porous network architecture and ultrathin interlinked nanowires acted as the skeleton of the aerogels were observed (Fig. 1B). Transmission electron microscope (TEM) images of PdBi aerogels were further confirmed the interlinked nanowires structure, exhibiting a uniform size distribution with an average diameter of approximately 5.8 nm (Fig. 1C). The protrusions allocated in the nanowires may be originated from the fusion of nanoparticles in the process of aerogel growth [7,9]. High resolution transmission electron microscopy (HRTEM) image manifested conspicuous lattice boundaries and abundantly exposed lattice fringes pervaded on the surface of nanowires (Fig. 1D), which are favorable for the improvement of catalytic activity. The interplanar distance of 0.22 nm and 0.19 nm were attributed to the (111) and (200) plane of fcc Pd, respectively, which were fit well with the selected area electron diffraction (SAED) pattern result presented in the inset of Fig. 1D. The X-ray photoelectron spectroscopy (XPS) spectrum (Fig. 1E) displayed that intermetallic PdBi were mainly included elemental components of Pd and Bi, coinciding with the energy-dispersive X-ray spectroscopy (EDS) data (Fig. S2 in Supporting information). The polycrystallinity of PdBi aerogels with different compositions was proved by the powder X-Ray diffraction (XRD) pattern (Fig. 1F). It can be found that the diffraction peak (111) plane was situated between the characteristic peak positions of fcc-structured Pd (JCPDS No. 46-1043) and Bi (JCPDS No. 44-1246). The diffraction peak was shifted to the position of fcc Pd with the decrease of Bi content (Fig. 1G), which is consistent with previously reported work [26,27].

As the same as the reported bimetallic alloy catalysts [28,29], the element components of Pd/Bi can be adjusted conveniently by modifying the molar ratio of Pd/Bi precursors. The composition of aerogels was identified by ICP-OES. The actual compositions of PdBi aerogels by varying the Pd/Bi molar ratio of the precursors were determined to be 86/14, 71/29, 59/41, 52/48 for Pd_4Bi_1, Pd_2Bi_1, Pd_1Bi_1, Pd_1Bi_2, respectively (Table S1 in Supporting information). This variation was attributed to that the standard reduction potential of $PdCl_4^{2-}$/Pd was higher than that of Bi^{3+}/Bi [30]. The Pd_4Bi_1, Pd_1Bi_1, and Pd_1Bi_2 aerogels were obtained by changing the Pd/Bi molar ratio of the precursors, respectively, and the nanowires network structure were also observed from their TEM images in Figs. S4A-C (Supporting information). As a control, polyvinylpyrrolidone (PVP)-capped PdBi composites exhibited nanowires structure, while they cannot form a hydrogel. Interestingly, for the pure Pd, no hydrogel was formed even after 1 day although the nanowires structure was also found in TEM image (Fig. S4E in Supporting information). For Monometallic Bi, hydrogel was also not formed. Its TEM image presented large and aggregated nanoparticles rather than ultrafine nanowires network (Fig. S4F in Supporting information).

XPS measurements were employed to ascertain valence states of PdBi aerogels. As presented in Fig. 2A, the valence state of Pd was mostly composed of metallic Pd (Pd^0), which can be assigned to peaks at 334.9 and 340.2 eV [31,32]. The peaks at 335.9 and 340.9 eV verified the Pd^{2+} in the sample [33], which can be ascribed to the surface oxidation during the synthesis procedure or sample storation. Notably, the metallic Pd peak of PdBi aerogels displayed a 0.5 eV negative shift compared to the pure Pd, indicating the existence of charge transfer from Bi to Pd and leading to the lowering of the d-band energy of Pd. As for the Bi element, the valence state of it primarily consists of Bi^{3+} which was assigned to the peaks at 158.7 and 164 eV. The binding energy at 156.8 and 162.1 eV corresponding to Bi $4f_{7/2}$ and Bi $4f_{5/2}$ confirmed the presence of Bi^0 (Fig. 2B). Such a phenomenon was also found in some reported work [34,35], which was probably because the amount of reduction of Bi^{3+} to metallic Bi was minimal.

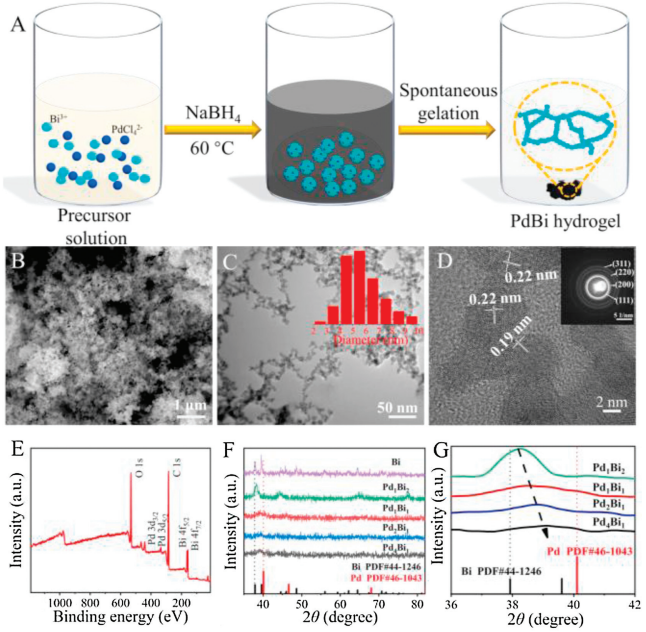

Fig. 1. (A) Schematic presentation of the preparation process of PdBi hydrogels, (B) SEM image and (C) TEM image of Pd_2Bi_1 aerogels (inset: size distribution of nanowires). (D) HRTEM image of Pd_2Bi_1 aerogels (inset: the SAED pattern). (E) Wide-scan XPS of PdBi aerogels. (F) XRD patterns of PdBi aerogels with different Pd/Bi ratios and (G) regional diffraction peak comparisons between the different components of PdBi aerogels.

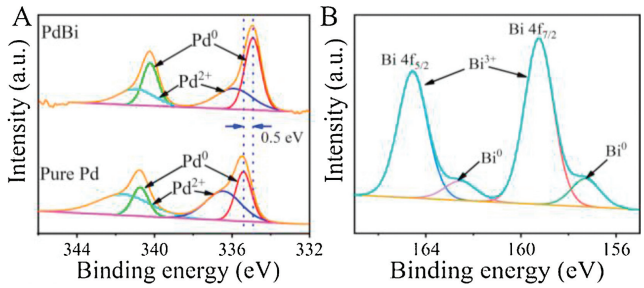

Fig. 2. The high-resolution XPS spectra of Pd 3d (A, top, PdBi aerogels, bottom, pure Pd) and Bi 4f (B).

The N_2 adsorption-desorption isotherms test for Pd_2Bi_1 aerogel have been conducted, the results indicated that the surface areas of Pd_2Bi_1 aerogel as estimated from Isotherm Linear Plot was 51.6 m^2/g (Fig. S5A in Supporting information). Based on the pore size distribution plot in Fig. S5B (Supporting information), adsorption average pore diameter of Pd_2Bi_1 aerogel was 21.5 nm. The high BET surface areas and wide pore distribution are advantageous for the mass transfer process during catalysis.

The reductive degradation of 4-NP and MB were selected as model reactions to assess the catalytic performances of PdBi aerogels. 4-NP is one of the priority pollutants because of its recalcitrance and harm to the human central nervous system [36]. However, its reduction product, 4-aminophenol (4-AP), has much lower toxicity [37]. The reduction of 4-NP simply by $NaBH_4$ was kinetically restricted but thermodynamically favorable due to the positive potential difference between 4-NP and BH_4^- molecules (ΔE = E(4-NP/4-AP) − E(H_3BO_3/BH_4^-) = 0.67 V) [38]. The 4-NP solution has an absorption at 316 nm. After addition of $NaBH_4$, the absorption peak was shifted to 400 nm assigned to 4-NPate ions (Fig. 3A). The color of the solution also was changed from light yellow to deep yellow. The peak intensity keeps constant even after 12 h, which means that the reduction cannot take place without catalysts (Fig. S6A in Supporting information). However, with the addition of intermetallic PdBi catalysts into the mixed solution, the yellow solution was bleached immediately, and a new absorption peak appeared at 298 nm attributed to the conversion of 4-NP to 4-AP. The peak intensity of 400 nm corresponding to 4-nitrophenolate ions decreased gradually along with the reduction proceeded (Fig. S7 in Supporting information). We have conducted the adsorption tests of 4-NP and MB by sole Pd_2Bi_1 aerogels with NaOH. As shown in Fig. S8 (Supporting information) the results indicated that either 4-NP or MB keep unchanged, which can be attributed to the trace amount of added PdBi aerogel is not inadequate to adsorb the 4-NP and MB, but exhibit highly effective catalytic performance for the reductive degradation of 4-NP and MB with the aiding of $NaBH_4$.

The whole reduction process was monitored by UV/vis spectra. The time-dependent spectra of 4-NP reduction (Fig. 3B) indicated that a small amount of Pd_2Bi_1 aerogels (20 μL, 1 mg/mL) will give rise to the fast conversion of 4-NP to 4-AP within 60 s. The peak intensity at 400 nm regularly decreased at a time interval of 20 s, indicating a highly efficient reduction performance of Pd_2Bi_1 aerogels towards 4-NP. In this reaction, the amount of $NaBH_4$ was large excess to that of 4-NP. Thus, the reaction could be considered independent of the $NaBH_4$ content. The catalytic reduction of 4-NP follows pseudo-first-order kinetics [39,40], the apparent rate constant (K_{app}) was determined by following equation: $\ln(C_t/C_0) = \ln(A_t/A_0) = -K_{app}t$. Where A_t and C_t is the absorbance and concentration of 4-NP at time t, A_0 and C_0 is the initial absorbance and concentration of 4-NP. K_{app} was calculated from the slope to be 0.0544 s^{-1} for Pd_2Bi_1 aerogels, which is considerably higher than that of some previously reported works [41–43]. The catalytic performances of the PdBi aerogels with different components were further investigated. The results indicated that the catalytic activity of Pd_2Bi_1 aerogel was remarkably higher than that of other aerogels. The K_{app} values were calculated to be 0.0196, 0.0106, 0.0052 s^{-1} for Pd_4Bi_1, Pd_1Bi_1, Pd_1Bi_2 aerogel, respectively (Figs. 3C and D). Besides K_{app}, another significant indicator of catalytic performance, turnover frequency (TOF), defined as the mole of nitrophenols per mole of the catalysts per hour, was introduced to compare with the catalysts in recent literature. As shown in Table S2 (Supporting information), the Pd_2Bi_1 aerogels exhibited the highest TOF value (1362 h^{-1}) among the as-prepared aerogels and other Pd-based and Bi-based catalysts. The negative effect of the surfactant on the catalytic performance of Pd_2Bi_1 aerogels was investigated. A commonly used surfactant, polyvinylpyrrolidone (PVP), was added into the precursor solution. It was found that the dispersed black solids instead of monolith hydrogels were obtained although the interlinked network was formed, and the PVP-Pd_2Bi_1 composition exhibited a terribly poor catalytic property compared to Pd_2Bi_1 aerogels. It is happy to see that even compared with commercial Pd/C, the rate constant of Pd_2Bi_1 aerogels was 4.2-fold higher than that of commercial Pd/C even though Pd amounts in the Pd/C was 50-fold than Pd_2Bi_1 aerogels. The catalytic efficiency of as-obtained PdBi aerogels was also dramatically better than that of monometallic Pd and Bi, which better verified that the unique network structure has a positive effect on the catalytic reduction (Fig. S9 in Supporting information).

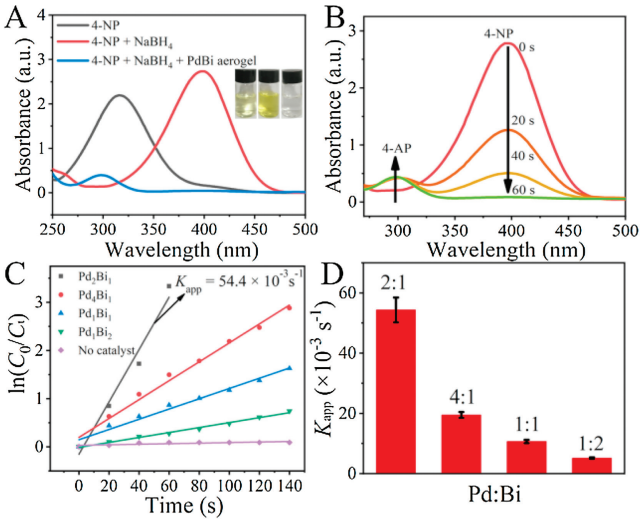

Fig. 3. (A) UV–vis spectra of 4-NP (inset, left), 4-NP + $NaBH_4$ (inset, middle) and after addition of PdBi aerogels (inset, right). (B) Time-dependent UV–vis spectra of 4-NP catalyzed by $NaBH_4$ in the presence of Pd_2Bi_1 aerogels. (C) Plot of $\ln(C_0/C_t)$ against the reaction time for PdBi aerogels with different Pd/Bi molar ratios, and without catalysts. (D) Comparison of apparent rate constant of PdBi aerogels with different Pd/Bi molar ratio. (All tests were conducted at 25 °C, and the concentration of PdBi aerogels was 0.011 mmol/L, the concentration of 4-NP was 0.25 mmol/L).

Similar to 4-NP reduction, MB solution has a strong absorption at 650 nm. The addition of excess aqueous $NaBH_4$ cannot degrade MB in the absence of intermetallic Pd_2Bi_1. Once upon with adding Pd_2Bi_1 aerogels, the blue solution discolored rapidly with its characteristic peak disappeared (Fig. 4A). The results proved that PdBi aerogels played an indispensable role in decreasing the activation energy of the reaction and exhibited efficient catalytic capability toward MB. The time-dependent UV/vis spectra indicated the high-performance Pd_2Bi_1 catalysts generated the rapid degradation of MB within 40 s (Fig. 4B). Analogous to 4-NP reduction, the degradation of MB also follows *pseudo*-first-order kinetics. According to the absorbance decrease at 650 nm, K_{app} can be estimated based on the slope of the regression. Accordingly, the K_{app} for Pd_2Bi_1 aerogels was calculated to be 0.0953 s^{-1}. The K_{app} of the aerogels with different Pd/Bi ratio were also determined to be 0.0374, 0.0161, 0.00381 s^{-1} for Pd_4Bi_1, Pd_1Bi_1, Pd_1Bi_2, respectively (Figs. 4C and D). TOF values of these catalysts for the degradation of MB were determined and listed in Table S2. Similarly, PVP-Pd_2Bi_1 composite, commercial Pd/C, monometallic Pd, and monometallic Bi were calculated to be 0.00838, 0.0154, 0.0127, 0.00411 s^{-1} (Fig. S10 in Supporting information), which were all inferior to that of Pd_2Bi_1 aerogels.

The high catalytic rate and TOF value were superior to the most reported Pd and Bi-based catalysts, which can be explained with the following reasons: (1) The unique structure of an advantageous 3D high-porosity system, free-standing bulk structure, ultrathin

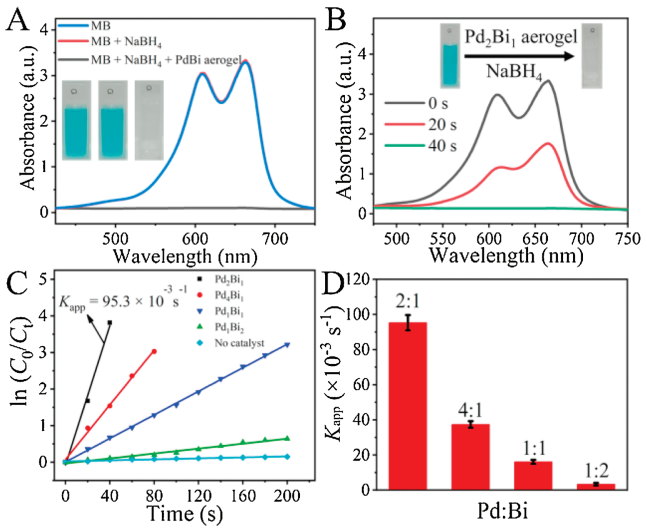

Fig. 4. (A) UV–vis spectra of MB (inset, left), MB + $NaBH_4$ (inset, middle) and after addition of PdBi aerogels (inset, right). (B) Time-dependent UV–vis spectra of MB catalyzed by $NaBH_4$ with Pd_2Bi_1 aerogels. (C) Plot of $\ln(C_0/C_t)$ against the reaction time for PdBi aerogels with different Pd/Bi molar ratios, and no catalysts. (D) Comparison of apparent rate constant of PdBi aerogels with different Pd/Bi molar ratios. (All tests were conducted at 25 °C, and the concentration of PdBi aerogels was 0.011 mmol/L, the concentration of MB was 0.15 mmol/L).

nanowires network acted as a reactor for speeding up the transfer and diffusion of substrates and products; (2) the pure metallic backbone and overall connectivity of aerogels afford sufficient active sites for reduction reaction, and the surfactant-free feature enables efficient electron transfer between catalysts and substrates; (3) bimetallic alloy can substantially improve catalytic performance by synergistic effect, which can significantly facilitate electronic relay, and in turn accelerate mass transfer process on the bimetallic surface.

The possible mechanism for the reduction of 4-NP and MB catalyzed by PdBi aerogels was illustrated in Scheme 1. The reduction of 4-NP by metal catalysts normally undergo three steps: (1) The BH_4^- and 4-NP species achieve adsorption equilibrium on the surface of catalysts; (2) electron transfer takes place from BH_4^- to 4-NP with the help of metallic active sites; (3) desorption of the product to form the catalytic cycle [44–46]. For our PdBi aerogels, bismuth has a lower work function than palladium, thus electrons transfer is accelerated on the intermetallic PdBi alloy interface by the formation of electron-rich/poor regions, which were also confirmed by XPS results. Furthermore, We tested the Cyclic Voltammetry (CV) for verifying the accelerated electrons transfer in 5.0 mmol/L $Fe(CN)_6^{3-}/Fe(CN)_6^{4-}$ solution containing 0.1 mol/L KCl, the results indicated the obvious amplification after modifying the Pd_2Bi_1 aerogel on the bare electrode (Fig. 11A in Supporting information). We also have conducted the electrochemical impedance spectroscopy (EIS) test for Pd_2Bi_1 aerogels, we compare the EIS results between the bare glassy carbon electrode (GCE) and modified Pd_2Bi_1 aerogels counterpart. As shown in Fig. S11B (Supporting information), it was generally known that the semicircle diameter of the EIS curve represents the resistance of electron transfer, while the linear part of the curve represents the charge diffusion process. When the Pd_2Bi_1 aerogels were modified on the electrode, the resistance (Ret) values decreased compared with the bare GCE, indicating that Pd_2Bi_1 aerogels had good conductivity for accelerating electron transfer. The HRTEM and XPS analysis of used Pd_2Bi_1 aerogel after reduction were conducted. As shown in Fig. S12 (Supporting information), the HRTEM image and XPS data indicated no obvious changes compared with that of fresh catalyst, which means the Pd_2Bi_1 aerogels were robust and can be as a desirable catalyst.

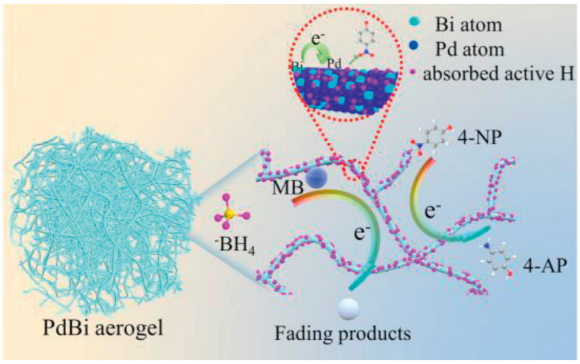

Scheme 1. The proposed mechanism for reduction of 4-NP and MB by $NaBH_4$ in the presence of PdBi aerogels.

In addition, when using borohydrides as a promising hydrogen source, the bimetallic surface gains many electrons from the borohydride ions, inducing the adsorption equilibrium of active hydrogen species on the surface of PdBi aerogels. Similarly, 4-nitrophenolate ions or MB molecules also reach adsorption equilibrium with pure intermetallic aerogels and are reduced by the active hydrogen species. Finally, poisonous pollutants are entirely converted into products with low toxicity and removed from the surface of aerogels to provide free and clean catalyst surface for the catalytic cycle [47,48].

In summary, PdBi bimetallic aerogels with three-dimensional interconnected nanowires network architecture and clear interfaces were prepared successfully by a one-step spontaneous gelation method. After optimization of the composition of the molar ratio of Pd and Bi precursors, Pd_2Bi_1 aerogels exhibit superior catalytic performance toward the reduction of 4-NP and MB. We believe that our method will pave a new avenue for rational design novel intermetallic aerogels based catalytic systems and broaden their applications beyond electrocatalysis.

Declaration of competing interest

The authors report no declarations of interest.

Acknowledgments

The authors would like to thank the financial support from the National Natural Science Foundation of China (Nos. 21245007 and 81000976), the Natural Science Foundation of Shandong Province (No. ZR2017MB017), Scientific Start-up Research Fund of Chengdu University of Information Technology (No. KYTZ201714) and the open fund of Innovation & Application Engineering Research Center for Mesoporous Materials of Shanxi Province (No. MMIA2019001). The author would like to thank Shiyanjia Lab (www.shiyanjia.com) for the XPS analysis. Yanfang Zhao was acknowledged for ICP-OES determination.

Appendix A. Supplementary data

Supplementary material related to this article can be found, in the online version, at doi:https://doi.org/10.1016/j.cclet.2020.09.043.

References

[1] W. Liu, A.K. Herrmann, N.C. Bigall, et al., Acc. Chem. Res. 48 (2015) 154–162.
[2] B. Cai, R. Hübner, K. Sasaki, et al., Angew. Chem. Int. Ed. 57 (2018) 2963–2966.
[3] B. Cai, A. Eychmüller, Adv. Mater. 31 (2019) 1804881.
[4] M. Luo, Y. Hong, W. Yao, et al., J. Mater. Chem. A 3 (2015) 2770–2775.
[5] L.A. Pretzer, K.N. Heck, S.S. Kim, et al., Catal. Today 264 (2016) 31–36.

[6] Q. Shi, C. Zhu, D. Du, et al., J. Mater. Chem. A 5 (2017) 19626–19631.
[7] Q. Shi, C. Zhu, H. Zhong, et al., ACS Energ. Lett. 3 (2018) 2038–2044.
[8] M. Oezaslan, W. Liu, M. Nachtegaal, et al., Phys. Chem. Chem. Phys. 18 (2016) 20640–20650.
[9] Q. Shi, C. Zhu, M. Tian, et al., Nano Energ. 53 (2018) 206–212.
[10] H. Wang, Y. Wu, X. Luo, et al., Nanoscale 11 (2019) 10575–10580.
[11] K. Iqbal, A. Iqbal, A.M. Kirillov, et al., J. Mater. Chem. A 6 (2018) 4515–4524.
[12] N. Sahiner, S. Yildiz, H. Al-Lohedan, Appl. Catal. B: Environ. 166 (2015) 145–154.
[13] M. Ismail, M. Khan, S.B. Khan, et al., J. Mol. Liq. 260 (2018) 78–91.
[14] S. Liu, X.L. Zhou, M.M. Zhang, et al., Chin. Chem. Lett. 27 (2016) 843–846.
[15] Z. Xiong, H. Zhang, W. Zhang, et al., Chem. Eng. J. 359 (2019) 13–31.
[16] H. Zhang, Q. Ji, L. Lai, et al., Chin. Chem. Lett. 30 (2019) 1129–1132.
[17] M. Zhu, L. Zhang, S. Liu, et al., Chin. Chem. Lett. 31 (2020) 1961–1965.
[18] F. Yu, L. Wang, Q. Xing, et al., Chin. Chem. Lett. 31 (2019) 1648–1653.
[19] Q. Li, X.Q. Qiao, Y. Jia, et al., ACS Appl. Nano Mater. 3 (2019) 68–76.
[20] K. Sahu, J. Singh, S. Mohapatra, Opt. Mater. 93 (2019) 58–69.
[21] S. Sarangapany, K. Mohanty, J. Alloys. Compd. 830 (2020) 154636.
[22] R. Das, V.S. Sypu, H.K. Paumo, et al., Appl. Catal. B: Environ. 244 (2019) 546–558.
[23] L. Qin, Z. Zeng, G. Zeng, et al., Appl. Catal. B: Environ. 259 (2019) 118035.
[24] A. Omidvar, B. Jaleh, M. Nasrollahzadeh, J. Colloid Interf. Sci. 496 (2017) 44–50.
[25] J. Song, Z.-F. Huang, L. Pan, et al., Appl. Catal. B: Environ. 227 (2018) 386–408.
[26] Y. Zhang, Y. Xia, S. Yan, et al., Dalton Trans. 47 (2018) 17461–17468.
[27] J. Ying, G. Jiang, Z.P. Cano, et al., Appl. Catal. B: Environ. 236 (2018) 359–367.
[28] W. Liu, P. Rodriguez, L. Borchardt, et al., Angew. Chem. Int. Ed. 52 (2013) 9849–9852.
[29] J. Zhang, G. Chen, D. Guay, et al., Nanoscale 6 (2014) 2125–2130.
[30] K.Y. Lee, Y.W. Lee, M. Kim, T.H. Kim, J. Mater. Chem. A 2 (2014) 2735–2741.
[31] R. Chen, M. Sun, G. Pang, et al., Chem. Electro. Chem. 4 (2017) 1081–1087.
[32] W. Hong, C. Shang, J. Wang, E. Wang, Energ. Environ. Sci. 8 (2015) 2910–2915.
[33] N. Ullah, M. Imran, K. Liang, et al., Nanoscale 9 (2017) 13800–13807.
[34] J. Wang, L. Tang, G. Zeng, et al., ACS Sustain. Chem. Eng. 5 (2016) 1062–1072.
[35] H. Xu, K. Zhang, B. Yan, et al., J. Power Sources 356 (2017) 27–35.
[36] X. Mei, J. Liu, Z. Guo, et al., J. Hazard. Mater. 363 (2019) 99–108.
[37] W. Gong, Q. Wu, G. Jiang, G. Li, J. Mater. Chem. A 7 (2019) 13449–13454.
[38] N. Bingwa, R. Meijboom, J. Phys. Chem. C 118 (2014) 19849–19858.
[39] T. Aditya, A. Pal, T. Pal, Chem. Comm. 51 (2015) 9410–9431.
[40] S. Wunder, F. Polzer, Y. Lu, et al., J. Phys. Chem. C 114 (2010) 8814–8820.
[41] K. Gu, X. Pan, W. Wang, et al., Small 14 (2018) 1801812.
[42] S. Li, Y. Yang, L. Liu, Q. Zhao, Chem. Eng. J. 334 (2018) 1691–1698.
[43] J. Gu, C. Hu, W. Zhang, A.B. Dichiara, Appl. Catal. B: Environ. 237 (2018) 482–490.
[44] W. Zhang, Y. Sun, L. Zhang, Ind. Eng. Chem. Res. 54 (2015) 6480–6488.
[45] C. Van Nguyen, S. Lee, Y.G. Chung, et al., Appl. Catal. B: Environ. 257 (2019) 117888.
[46] S. Fountoulaki, V. Daikopoulou, P.L. Gkizis, et al., ACS Catal. 4 (2014) 3504–3511.
[47] M. Kohantorabi, M.R. Gholami, Ind. Eng. Chem. Res. 56 (2017) 1159–1167.
[48] Y. Khalavka, J. Becker, C. Sonnichsen, J. Am. Chem. Soc. 131 (2009) 1871–1875.